

RF Cavities II

Salvador Sosa Güitrón

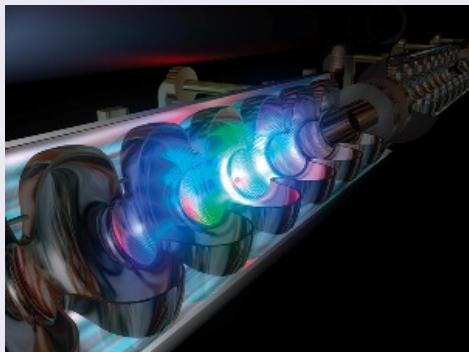
Old Dominion University
Mexican Particle Accelerator School 2015
Guanajuato, Mexico



- 1 Why Superconducting RF?
- 2 SRF Fundamentals
 - Superconductivity
- 3 SRF Technology
 - Cavity Fabrication
 - Cavity Testing
 - Loss Mechanisms
 - Cavity Processing
- 4 Recent Breakthroughs
 - Alternatives to Nb
 - Multilayers
 - N doping
- 5 Final Comments

Why Superconducting RF cavities?

- **Low power dissipation**
 - High gradient in CW or long-pulsed operation
 - Less number of cavities (less beam disruption)
 - Shorter accelerator (cost saving)
 - Cavity design with large beam tube
 - Beam stability
 - Higher beam current





INPUT

SL17

WARNING

ISAC II





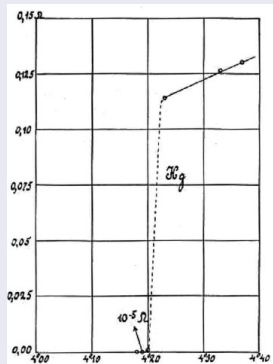
Jefferson Lab
100MHz 6-cell high beta cavity prototype
Spallation Neutron Source (SNS), built by JLAB

Jefferson Lab
1.3 GHz Large Grain 3-cell cavity
E.C. built by JLAB

- 1 Why Superconducting RF?
- 2 SRF Fundamentals
 - Superconductivity
- 3 SRF Technology
 - Cavity Fabrication
 - Cavity Testing
 - Loss Mechanisms
 - Cavity Processing
- 4 Recent Breakthroughs
 - Alternatives to Nb
 - Multilayers
 - N doping
- 5 Final Comments

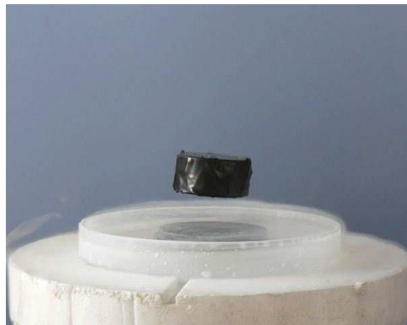
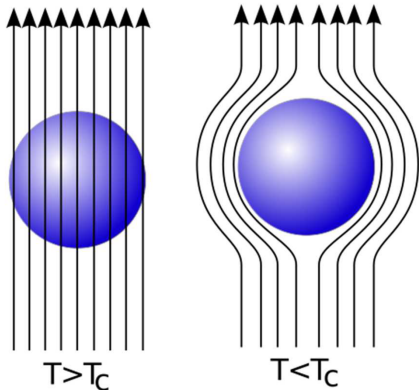
Superconductivity

- Discovered by Kamerlingh Onnes in 1911
- Drop to zero in electric resistance of Hg at 4.2 K



Complete Diamagnetism

- Magnetic field expulsion from the material below T_c (Meissner state)

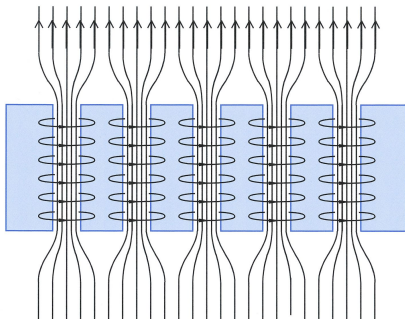


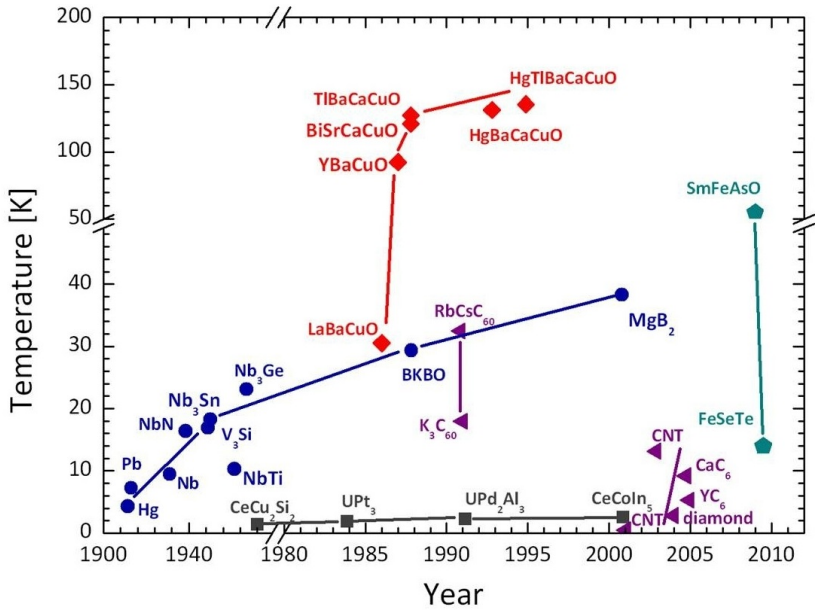
- For SRF applications operate in the Meissner state

Magnetic Flux Quantization

- Quantization of the flux field
- Type-II superconductors
- $\Phi_0 = 2.067 \cdot 10^{-15} \text{ Wb}$

$$\Phi = n \cdot \Phi_0$$





2-fluid model of Superconductivity

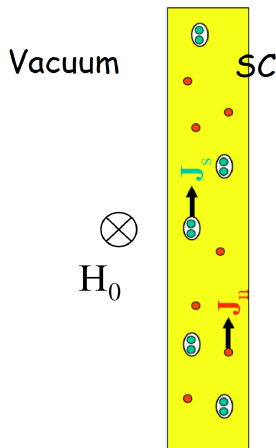
- Current density in the metal has a normal and superconducting component:

$$J = J_N + J_{SC}$$

- The number of normal electrons increases with T as:

$$N(e) \propto e^{-\Delta/k_B T}$$

- 2Δ is the superconducting energy gap.



G. Ciovatti

London equations (I)



F. and H. London, 1935

- Superelectrons accelerate steadily in the presence of a constant electric field

$$m \frac{d\vec{v}_s}{dt} = e\vec{E} \quad \begin{array}{c} \text{blue arrow pointing right} \\ \uparrow \\ J_s = n_s e v_s \end{array} \quad \frac{d\vec{J}_s}{dt} = \frac{n_s e^2}{m} \vec{E}$$

$$\lambda_L = \sqrt{\frac{m}{\mu_0 n_s e^2}}$$

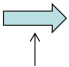
London penetration depth

$$\frac{d\vec{J}_s}{dt} = \frac{1}{\mu_0 \lambda_L^2} \vec{E}$$

- $\mathbf{E}=0$: J_s goes on forever
- \mathbf{E} is required to maintain an AC current

London equations (II)

$$\vec{\nabla} \times \vec{J}_s = \frac{1}{\mu_0 \lambda_L^2} \vec{\nabla} \times \vec{E} \quad \vec{\nabla} \times \vec{J}_s = -\frac{1}{\mu_0 \lambda_L^2} \dot{\vec{B}}$$




$$\vec{\nabla} \times \vec{E} = -\dot{\vec{B}}$$

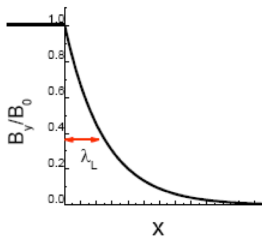
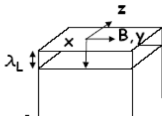
$$\vec{\nabla} \times \vec{J}_s = -\frac{1}{\mu_0 \lambda_L^2} \vec{B}$$

- **B** is the source of J_s
- Spontaneous flux exclusion

$$\vec{\nabla} \times \vec{B} = \mu_0 \vec{J}_s \longrightarrow$$



$$\nabla^2 \vec{B} = \frac{\vec{B}}{\lambda_L^2}$$



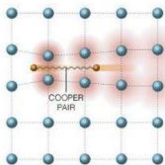
Theory of Superconductivity (BCS)

- Attractive interaction between free electrons, mediated by lattice phonons.



J. Bardeen, L. Cooper, R. Schrieffer, *Phys. Rev.* **108**, 1175, 1957.

Cooper pairs

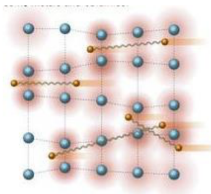


- Positively charged wake due to moving electron attracting nearby atoms
- This wake can attract another nearby electron

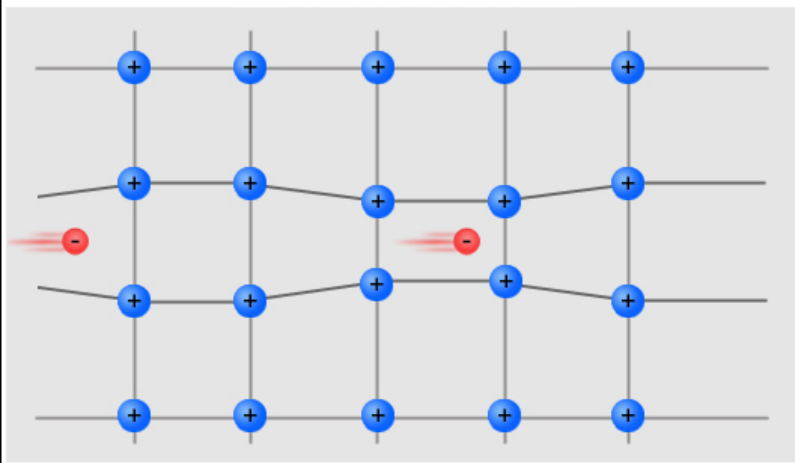


a Cooper pair is formed

- Cooper pairs are formed by electrons with opposite momentum and spin
- Cooper pairs belong all to the same quantum state and have the same energy
- When carrying a current, each Cooper pair acquires a momentum which is the same for all pairs
- The **total** momentum of the pair remains constant. It can be changed only if the pair is broken, but this requires a minimum energy 2Δ



Cooper pairs make super conductors



At extremely low temperatures, an electron can draw the positive ions in a superconducting material towards it. This movement of the ions creates a more positive region that attracts another electron to the area.

Characteristic Lengths

- **Coherence length** $\xi_0 \equiv \frac{\hbar v_F}{\pi \Delta(0)}$: interaction distance between electrons forming a Cooper pair $\xi_0 = 39 \text{ nm for Nb}$
- **Penetration depth**, $\lambda(T)$: decay length of magnetic field in the superconductor $\lambda(0) = 36 \text{ nm for Nb}$

$$\lambda(T) = \frac{\lambda_L(0)}{\sqrt{1 - \left(\frac{T}{T_c}\right)^4}}$$

Effect of impurities on ξ and λ

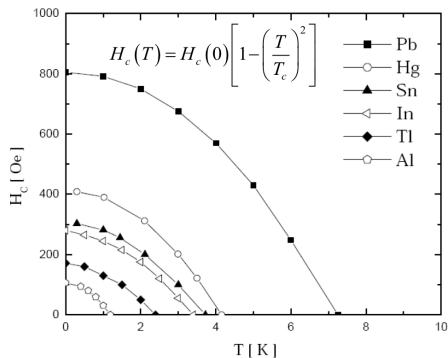
- Adding impurities to a superconductor reduces the normal electrons mean free path, so that the electrodynamic response changes from “**clean**” ($l \gg \xi$) to the “**dirty**” limit ($l \ll \xi$).
- Changes in the characteristic lengths of the SC can be approximated as:

$$\frac{1}{\xi} = \frac{1}{\xi_0} + \frac{1}{l}$$

$$\lambda(l, T) = \lambda_L(T) \sqrt{1 + \frac{\xi_0}{l}}$$

Thermodynamic Critical Field

Superconducting state lost above a critical value H_c of magnetic field

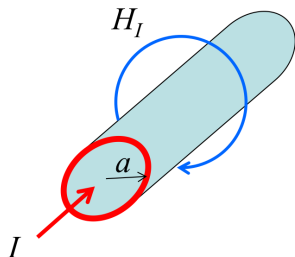


From BCS theory:

$$H_c(0) = \sqrt{\frac{0.472\gamma}{\mu_0}} T_c$$

Critical current

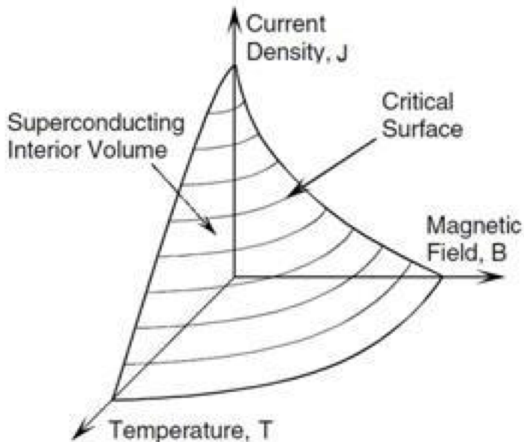
Superconductivity is lost when a current flowing in a SC increases above a critical value.



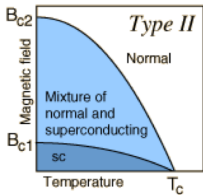
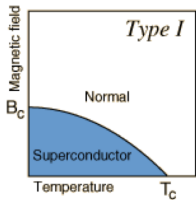
$$I_c = 2\pi a H_c$$

$$J_c = \frac{H_c}{\lambda}$$

Phase diagram of SC

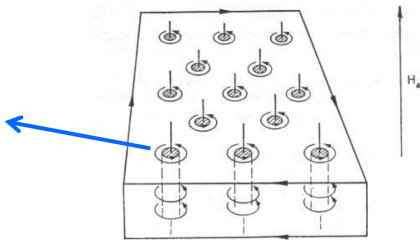
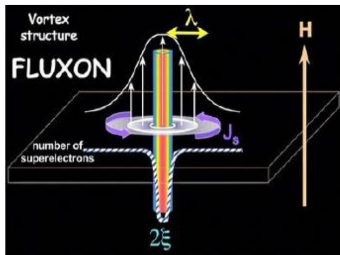


Type-I and Type-II SC

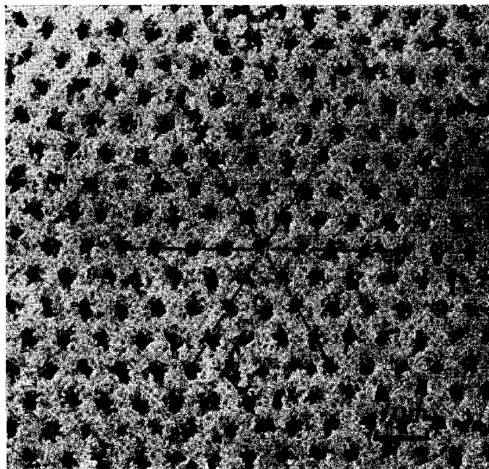


Abrikosov found solutions $\psi(x, y)$ with periodic zeros = lattice of vortices with **quantized magnetic flux**

$$\Phi_0 = \frac{h}{2e} = 2.07 \times 10^{-15} \text{ Wb}$$



Flux-line lattice



Triangular flux-line lattice penetrating the top surface of a SC lead-indium sample

The points of exit of the flux lines are decorated by small ferromagnetic particles

H. Träuble and U. Essmann, *J. Appl. Phys.* **39**, 4052 (1968);

Critical fields

$$H_c = \frac{\phi_0}{2\pi\sqrt{2}\lambda\xi} \quad \text{Thermodynamic critical field}$$

$$H_{c2} = \sqrt{2}\kappa H_c = \frac{\phi_0}{2\pi\xi^2} \quad \text{Upper critical field}$$

$$H_{c1} \approx \frac{\phi_0}{4\pi\lambda^2} \ln(\kappa + \alpha) \quad \text{Lower critical field}$$

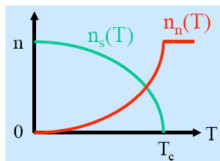
$$\alpha = \frac{1}{2} + \frac{1 + \ln 2}{2\kappa - \sqrt{2} + 2} = \begin{cases} 1.35, \kappa = 0.71 \\ 0.5, \kappa \gg 1 \end{cases}$$

For Nb, $\kappa \sim 0.85$, $B_{c1}(0) \sim 180$ mT, $B_c(0) \sim 195$ mT, $B_{c2}(0) \sim 400$ mT

Surface resistance of superconductor

$$R_s = \frac{1}{2} \mu_0^2 \omega^2 \sigma_1 \lambda_L^3$$

- $R_s \propto \omega^2 \rightarrow$ use low-frequency cavities to reduce power dissipation
- Temperature dependence:



$$n_s(T) \propto 1 - (T/T_c)^4$$

$$\sigma_1(T) \propto n_n(T) \propto e^{-\Delta/k_B T}$$

$$R_s \propto \omega^2 \lambda_L^3 l \exp(-\Delta/k_B T)$$

$$T < T_c/2$$

Material purity dependence of R_s

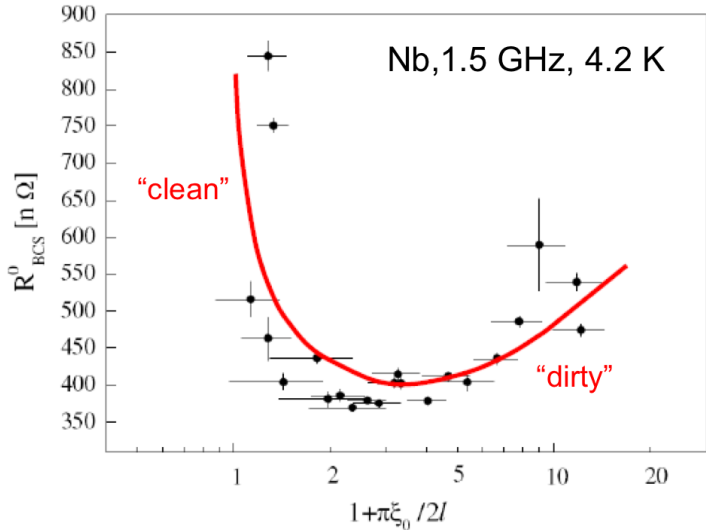
- The dependence of the penetration depth on l is approximated as

$$\lambda(l) \approx \lambda_L \sqrt{1 + \frac{\xi_0}{l}}$$

- $\sigma_1 \propto l$

$$\begin{aligned} \Rightarrow R_s \propto \left(1 + \frac{\xi_0}{l}\right)^{3/2} l & \Rightarrow R_s \propto l & \text{if } l \gg \xi_0 \text{ ("clean" limit)} \\ & R_s \propto l^{-1/2} & \text{if } l \ll \xi_0 \text{ ("dirty" limit)} \end{aligned}$$

R_s has a minimum for $l = \xi_0/2$



C. Benvenuti et al., Physica C **316** (1999) 153.

BCS surface resistance (2)

- There are numerical codes (Halbritter (1970)) to calculate R_{BCS} as a function of ω , T and material parameters (ξ_0 , λ_L , T_c , Δ , l)
- For example, check <http://www.lepp.cornell.edu/~liepe/webpage/researchsrimp.html>
- A good approximation of R_{BCS} for $T < T_c/2$ and $\omega < \Delta/\hbar$ is:

$$R_{\text{BCS}} \cong \frac{\mu_0^2 \omega^2 \lambda^3 \sigma_n \Delta}{k_B T} \ln \left[\frac{C_1 k_B T}{\hbar \omega} \right] \exp \left[-\frac{\Delta}{k_B T} \right] \quad C_1 = 2.246$$

Let's run some numbers: Nb at 2.0 K, 1.5 GHz $\rightarrow \lambda = 36$ nm, $\sigma_n = 3.3 \times 10^8$ 1/ Ω m, $\Delta/k_B T_c = 1.85$, $T_c = 9.25$ K

$$R_{\text{BCS}} \cong 20 \text{ n}\Omega$$

$$X_s \cong 0.47 \text{ m}\Omega$$

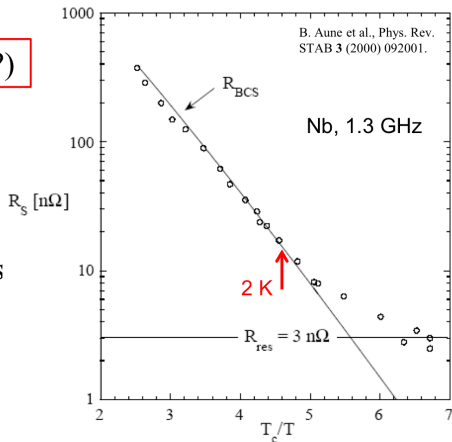
$$\begin{aligned} \text{Nb} &\rightarrow \frac{R_{\text{BCS}}(2 \text{ K}, 1.5 \text{ GHz})}{R_s(300 \text{ K}, 1.5 \text{ GHz})} \cong 2 \times 10^{-6} \\ \text{Cu} &\rightarrow \end{aligned}$$

Residual resistance

$$R_s = R_{\text{BCS}}(\omega, T, \Delta, T_c, \lambda_L, \xi_0, l) + R_{\text{res}}(?)$$

Possible contributions to R_{res} :

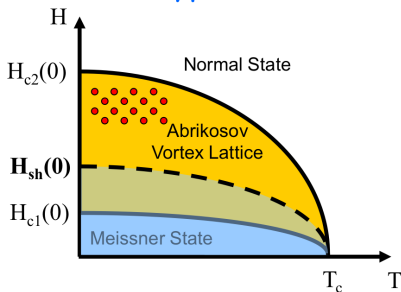
- Trapped magnetic field
- Normal conducting precipitates
- Grain boundaries
- Interface losses
- Subgap states



For Nb, R_{res} (~ 1 - $10 \text{ n}\Omega$) dominates R_s at low frequency ($f < \sim 750 \text{ MHz}$) and low temperature ($T < \sim 2.1 \text{ K}$)

RF critical field: superheating field

Type-II SC



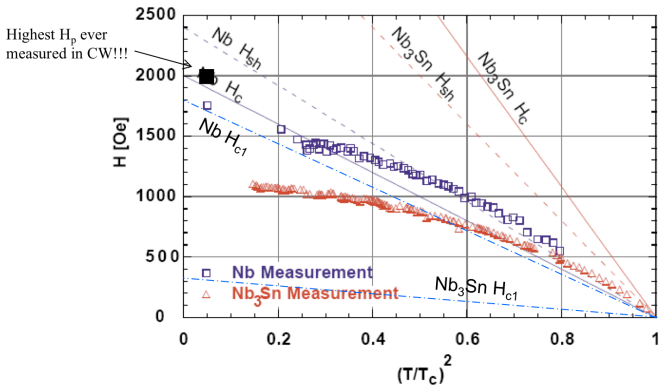
- Penetration and oscillation of vortices under the RF field gives rise to strong dissipation and the surface resistance of the order of R_s in the normal state
- the Meissner state can remain metastable at higher fields, $H > H_{c1}$ up to the superheating field H_{sh} at which the Bean-Livingston surface barrier for penetration of vortices disappears and the Meissner state becomes unstable

H_{sh} is the maximum magnetic field at which a type-II superconductor can remain in a true non-dissipative state not altered by dissipative motion of vortices.

At $H = H_{sh}$ the screening surface current reaches the depairing value $J_d = n_s e \Delta / p_F$

Superheating field: experimental results

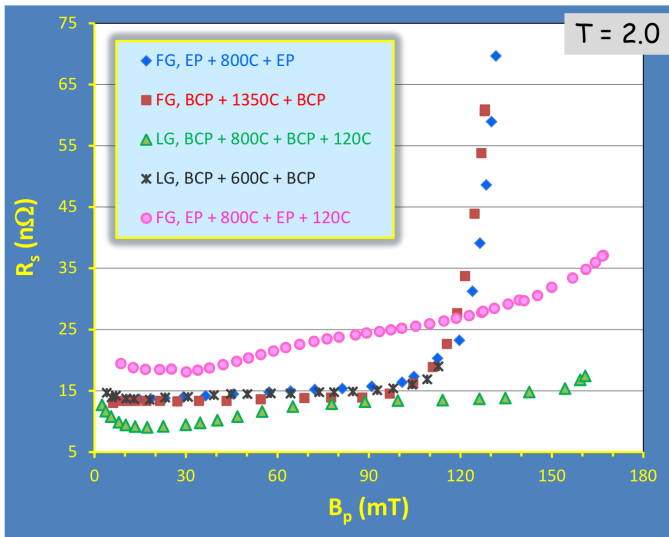
- Use high-power (~ 1 MW) and short (~ 100 μ s) RF pulses to achieve the metastable state before other loss mechanisms kick-in



T. Hays and H. Padamsee, Proc. 1997 SRF Workshop, Abano Terme, Italy, p. 789 (1997).

- RF magnetic fields higher than H_{c1} have been measured in both Nb and Nb₃Sn cavities. However max H_{RF} in Nb₃Sn is \ll predicted H_{sh} ...

Field dependence of R_s : Experimental results



FG: fine grain Nb
LG: large grain Nb

BCP: buffered
chemical polishing
EP: electropolishing

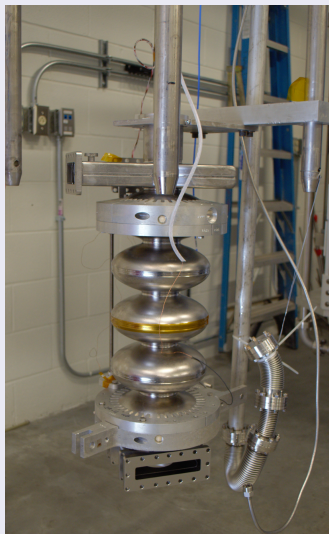
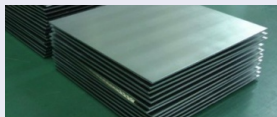
800C, 600C, 1350C,
120C: heat treatment
temperatures

B. Aune et al., Phys. Rev. STAB 3 (2000) 092001.
R. Geng, SRF11, p. 74
G. Ciovati, P. Kneisel and G. Myneri, SSTINIO, p. 25.
W. Singer et al., Phys. Rev. ST. Accel. Beams 16 (2013) 012003

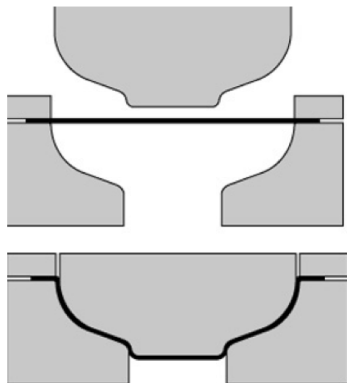
- 1 Why Superconducting RF?
- 2 SRF Fundamentals
 - Superconductivity
- 3 SRF Technology
 - Cavity Fabrication
 - Cavity Testing
 - Loss Mechanisms
 - Cavity Processing
- 4 Recent Breakthroughs
 - Alternatives to Nb
 - Multilayers
 - N doping
- 5 Final Comments

Niobium

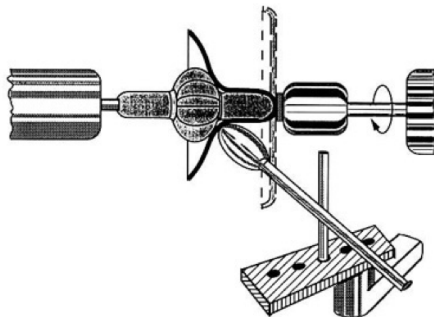
- $T_c \simeq 9.1$ K
- $H_c \simeq 200$ mT
- Chemically inert
- Easy to machine



Cavity Fabrication



(a)

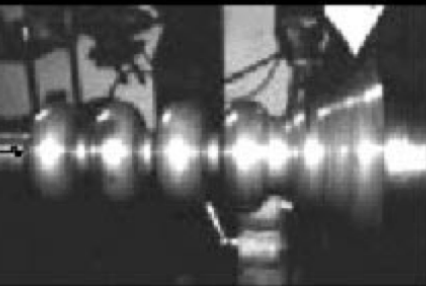
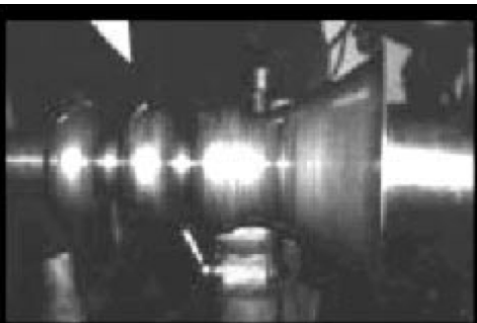


(b)

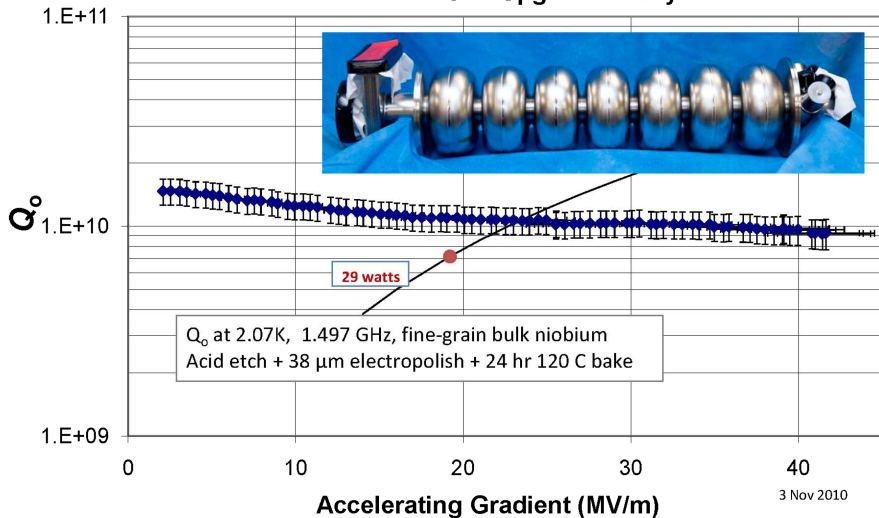
Figure: a) Deep drawing and b) single-sheet spinning.



Figure: Dice for half cell elliptical cavity deep pressing.



7-cell CEBAF 12 GeV Upgrade Cavity



Q-slopes

Low-field Q-slope

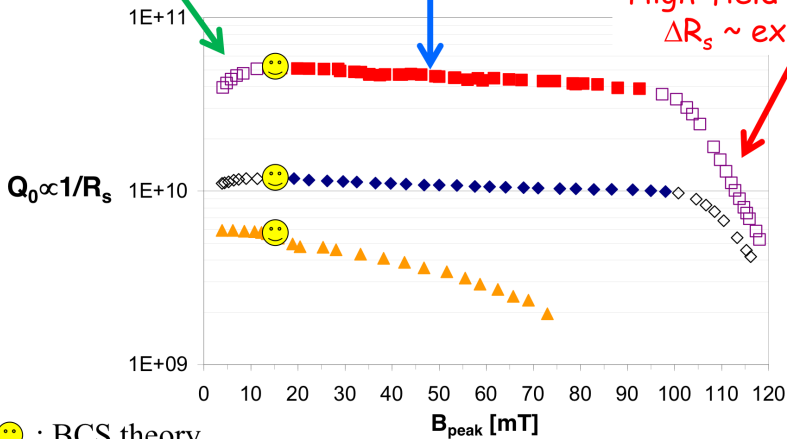
$$\Delta R_s \sim -\alpha/H^2$$

Medium-field Q-slope

$$\Delta R_s \sim R_1 H + \gamma H^2$$

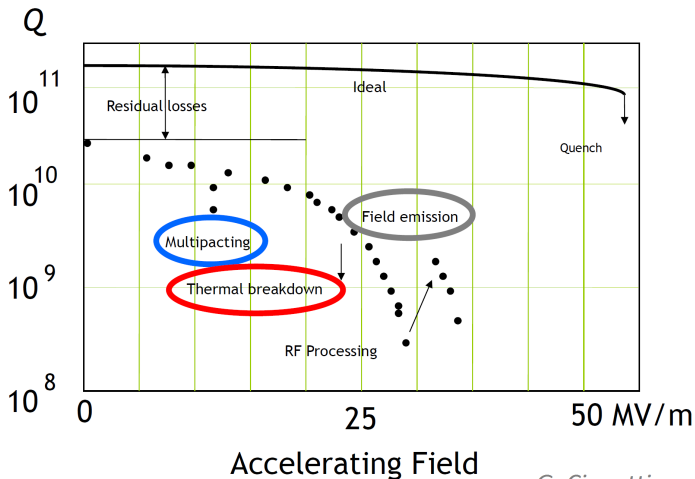
High-field Q-slope

$$\Delta R_s \sim \exp(\beta H)$$



☺ : BCS theory

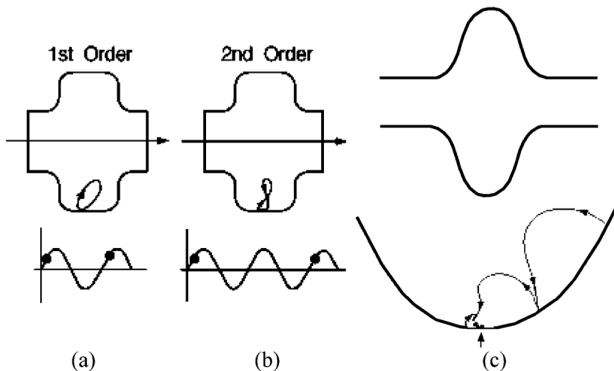
Performance limitations



G. Ciovatti

Multipacting and Choice of Geometry

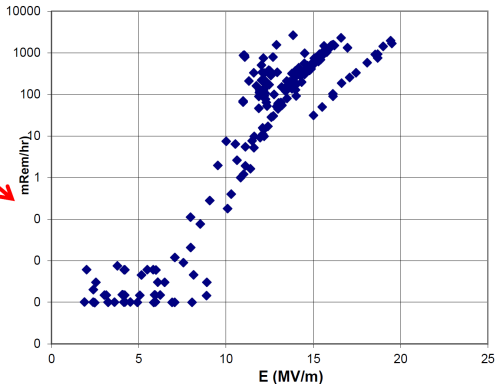
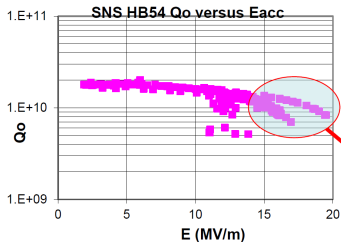
- Resonant process in which secondary electrons are generated, absorbing input power and hitting the surface of the cavity.
- Acts as a potential barrier and is present only at certain frequencies.



Field Emission

- Characterized by an exponential drop of the Q_0
- Associated with production of x-rays and emission of dark current

SNS HTB 54 Radiation at top plate versus Eacc 5/16/08 cg



Field Emitters

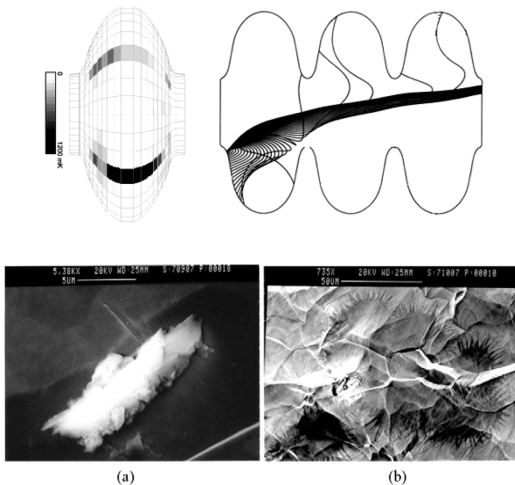


Figure: a) SEM micrograph of a particle purposely left in the Nb cavity. b) Same site shown after applying an RF field of 75 MV/m.

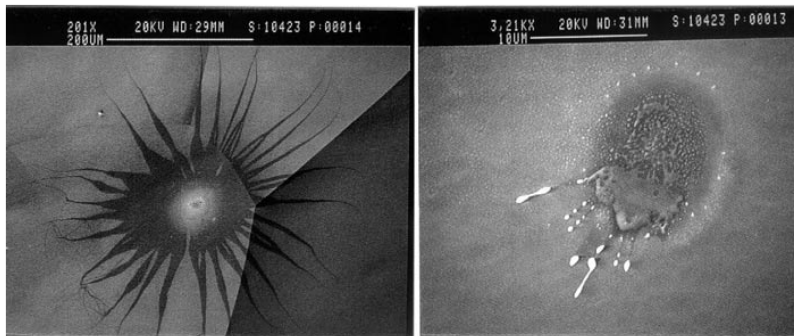


Figure: a) SEM micrograph of a starburst at a processed defect site and b) zoom into the center region, In was identified at this location.

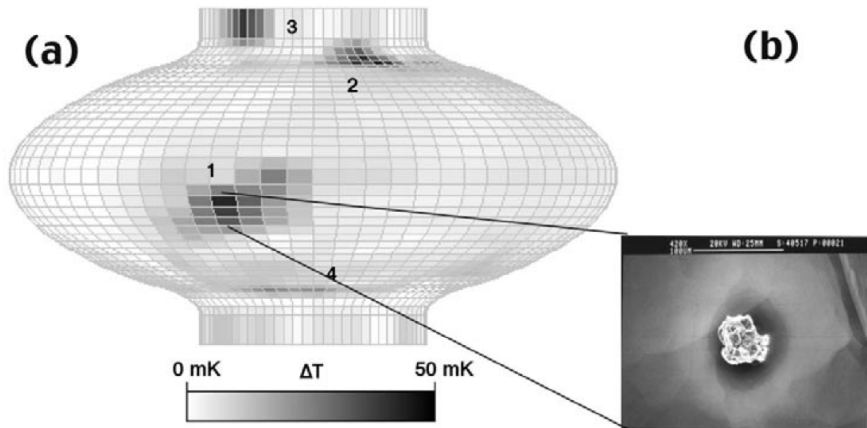


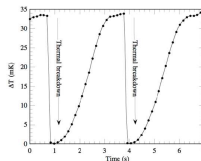
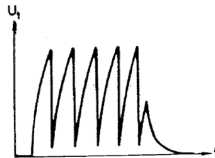
Figure: a) Temperature mapping of a 1.5 GHz cavity, a temperature increment is observed in region 1 due to thermal breakdown. Locations 2,3,4, correspond to field emission. b) SEM micrograph at site 1 shows a defect: Cu particle partially melted in Nb.

Limits the maximum magnetic field to be excited in the surface of the cavity.

- Originated in surface defects, order size is millimeters.
- When the local temperature at some defect location exceeds T_c of the superconductor, power losses increase significantly.
- As more regions lose superconductivity, thermal breakdown increases; thus decreasing the quality factor of the cavity.

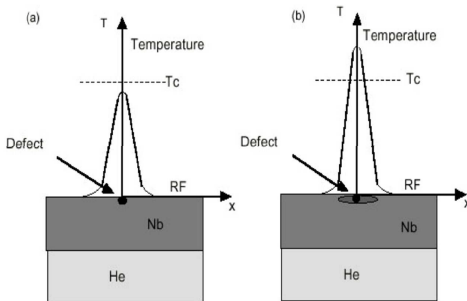
Symptom of Quench

- Sudden collapse (ms time scale) of field in SRF cavity
 - Field may self recovers
 - Or may not
- Detection of temperature rise at cavity wall near quench source
 - Can be as high as a few K



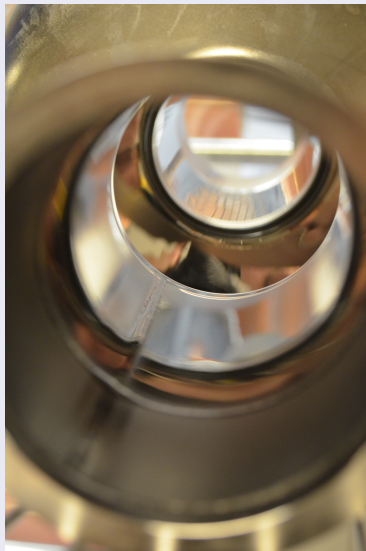
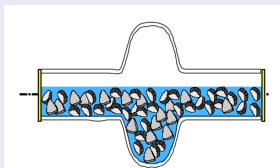
Physics of Thermal Quench

- Power dissipation in **normal conducting defect** generates heat $\frac{dP_c}{ds} = \frac{1}{2} R_s |\mathbf{H}|^2$. $R_s \begin{cases} n\Omega, \text{ s.c.} \\ m\Omega, \text{ n.c.} \end{cases}$
- Poor thermal conductivity of superconducting wall limits heat conduction
- This causes **temperature rise to exceed T_c (9.25 K) in surrounding superconducting region**
- This causes additional resistive heating
- The **normal conducting region grows** rapidly, leading to quench



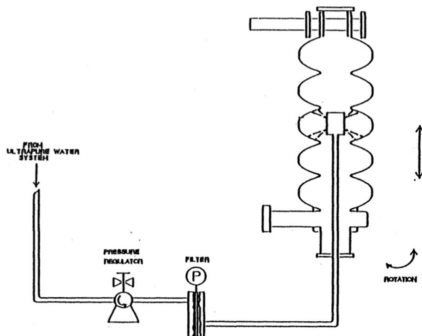
Centrifugal Barrel Polishing

- Reduction in the needed quantity of hazardous chemicals
- Simple technology and inexpensive



Cavity Processing: High Pressure Rinse

- De-ionized water, 18 M Ω -cm resistivity
- 1300 PSI pressure



Courtesy P. Kneisel

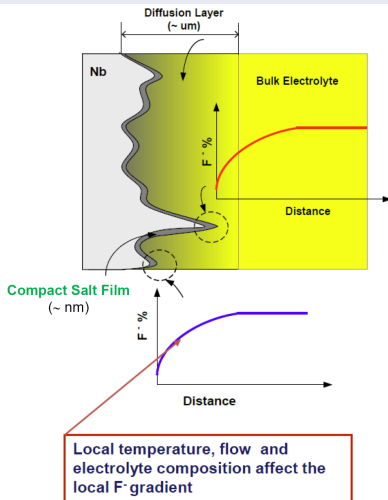
Buffered Chemical Polishing

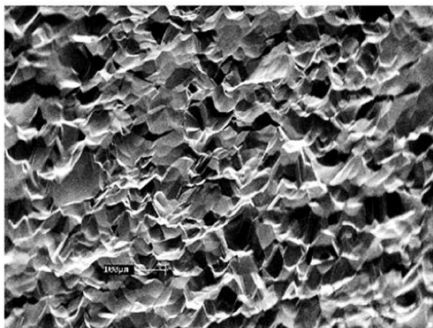
- Etches Nb surface, removing impurities and reducing the risk of thermal breakdown.
- HF : HNO₃ : H₃PO₄ at 1:1:2
- Control the reaction through the acid temperature.
- Removal rate of 1 $\mu\text{m}/\text{min}$



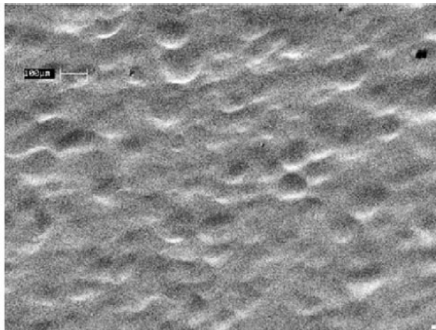
Electro-Polishing

- HF : H₂SO₄ at 1:9
- Anodization of Nb in H₂SO₄ forces growth of Nb₂O₅
- F⁻ in HF dissolves Nb₂O₅
- Removal rate of 0.4 μm/min
- Overall, a most homogeneous surface





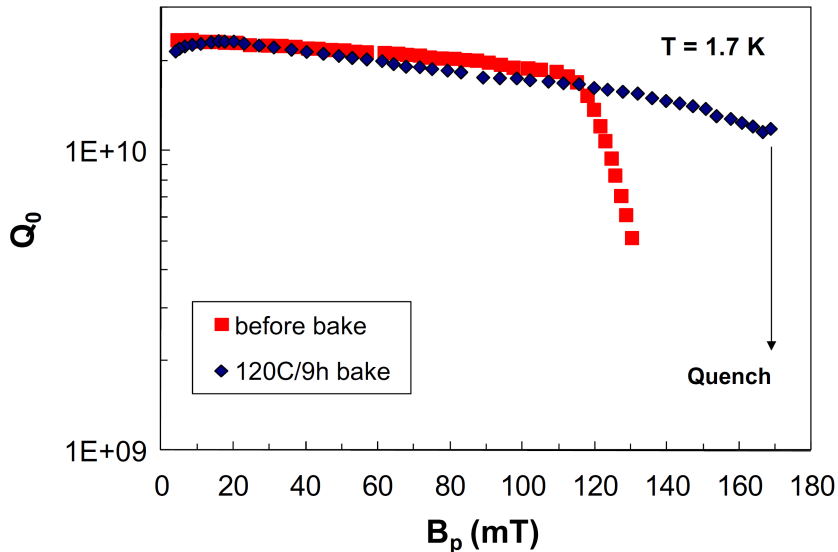
(a)



(b)

Figure: Micrograph comparison between a Nb surface processed by a) BCP and b) EP.

Low Temperature Baking



Clean Room

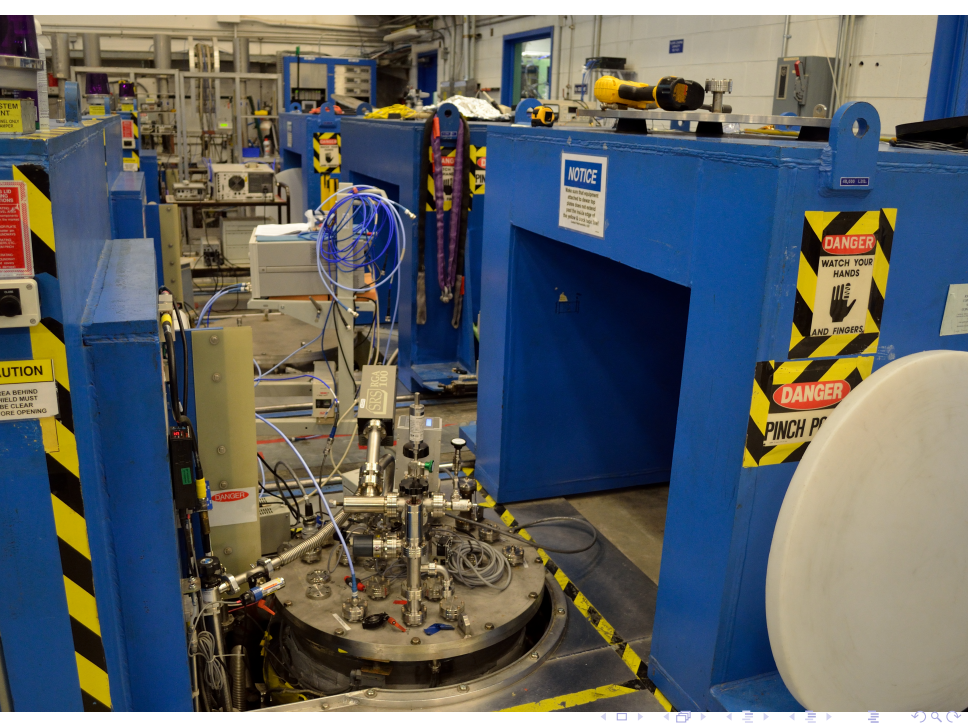
- Laminar flow of air keeps particles away from SRF components
- Strict protocols of operation inside the Clean Room
- Users are the most considerable source of contamination





Vertical and Horizontal Testing

- Vertical Testing
 - Material
 - Fabrication Techniques
 - Preparation recipe
- Horizontal Testing
 - Power couplers
 - High Order Mode absorbers
 - Cryomodule



NOTICE
Please do not touch the
machine to clean the
area. Please do not touch
the machine while it is
running. Do not touch the
machine if you are not
trained. Do not touch the
machine if you are not
trained. Do not touch the
machine if you are not
trained.

DANGER
WATCH YOUR
HANDS
AND FINGERS

DANGER
PINCH POINT

CAUTION
AREA BEHIND
FIELD MUST
BE CLEAR
BEFORE OPENING

DANGER

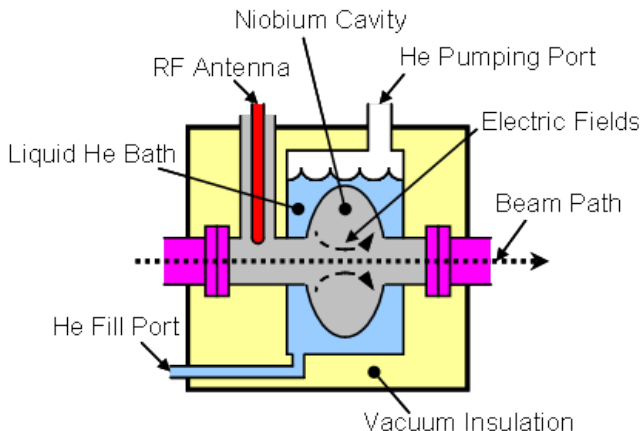
STS
100



BLU-100

Cavity in a Cryogenic Module

- A cryogenic module is the final container of the cavity, ready for transportation and installation at an accelerator facility.
- Dewar, used in Jlab's Vertical Test Area.





- 1 Why Superconducting RF?
- 2 SRF Fundamentals
 - Superconductivity
- 3 SRF Technology
 - Cavity Fabrication
 - Cavity Testing
 - Loss Mechanisms
 - Cavity Processing
- 4 Recent Breakthroughs
 - Alternatives to Nb
 - Multilayers
 - N doping
- 5 Final Comments

Alternate SRF materials to Nb

	T_c [K]	B_c [mT]	B_{c1} [mT]	λ [nm]
Nb	9.2	200	170	40
Nb ₃ Sn	18	540	40	85
NbN	16.2	230	20	200
MgB ₂	40	320	20-60	140
Ba _{0.6} K _{0.4} Fe ₂ As ₂	38	500	30	200

Table: Superconducting properties of attractive SRF materials.

R_s comparison of different materials

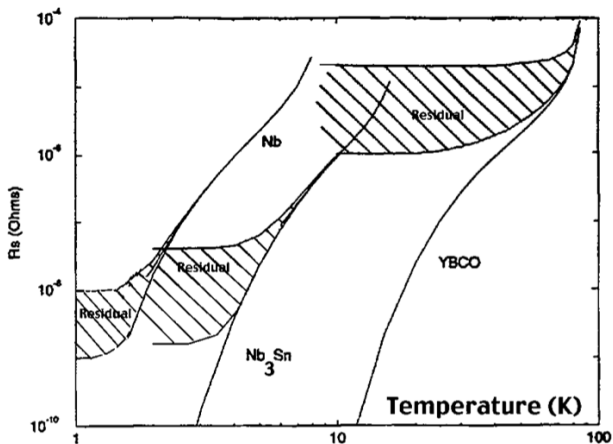
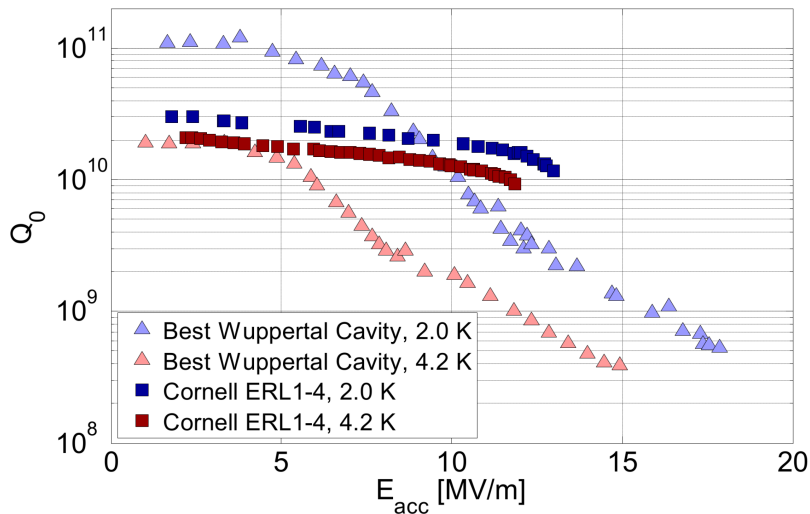


Figure: R_s for Nb, Nb₃Sn and High T_c ceramic.

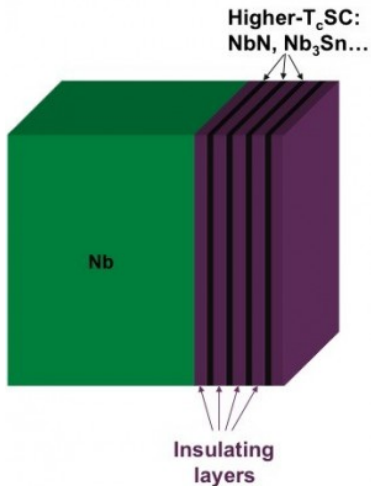
Nb₃Sn Cavities



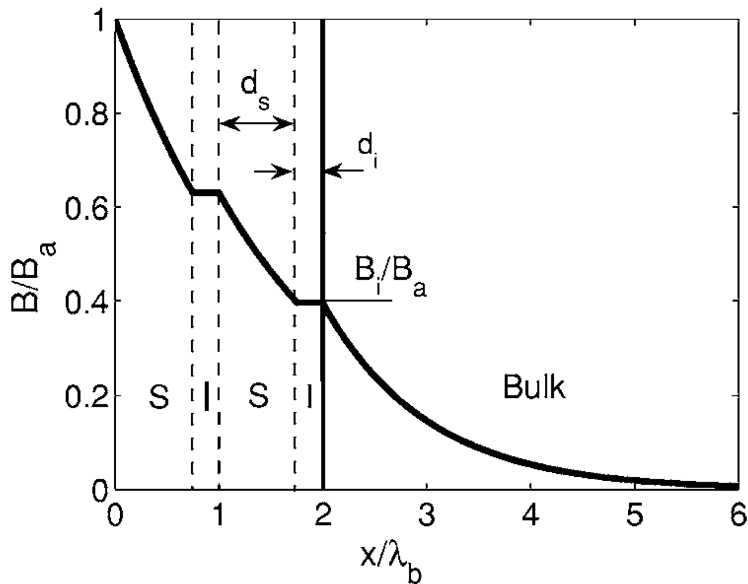
S. Posen, M. Liepe, *Proc. PAC 2013, THOBA2*

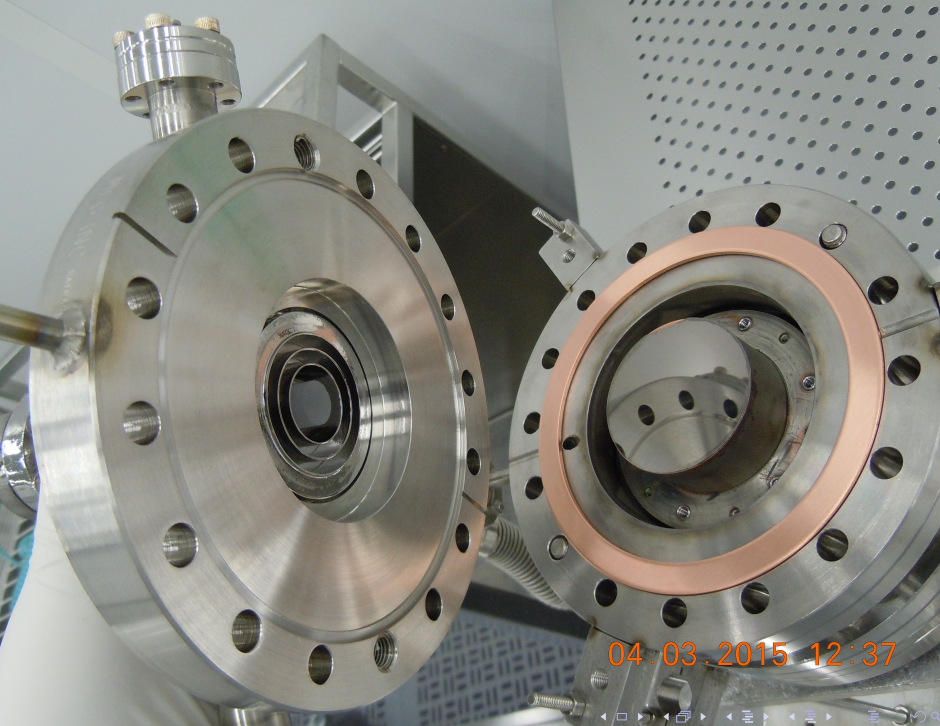
Multilayer Structures

- Field enhancement of Nb by thin films of high T_c superconductors



Multilayer Structures II



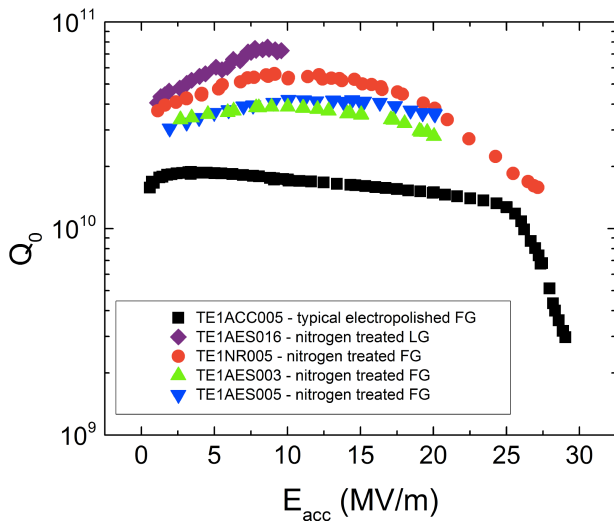


04.03.2015 12:37

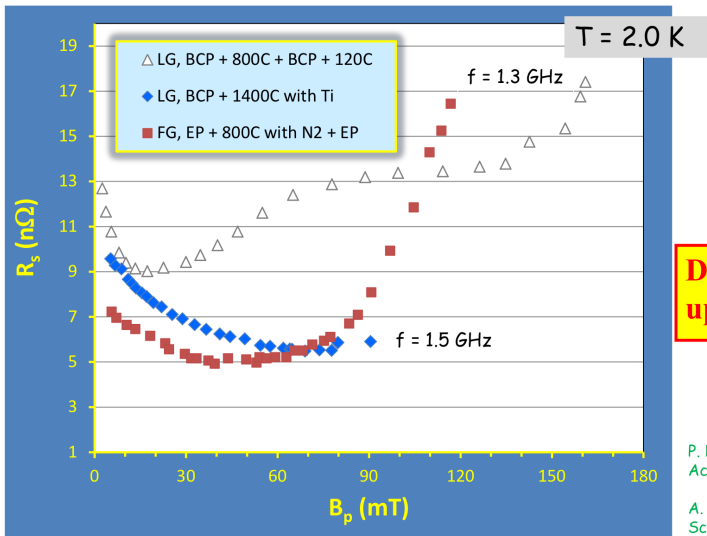


Nitrogen Doping

- Cavity baking with N_2 , followed by BCP:



Recent breakthroughs...



**Decreasing $R_s(H)$
up to ~90 mT**

P. Dhakal et al., Phys. Rev. ST
Accel. Beams **16** (2013) 042001

A. Grassellino et al., Supercond.
Sci. Tech. **26** (2013) 102001

Active research in:

- Elliptical cavities for particle acceleration
- Low β and deflecting cavities
- LCLS-2 Cryomodules
- Superconducting films as alternatives to bulk Nb
- High Q performance



- Steady progress in SRF science and technology over the last few decades
- More than proven and reliable technology
- More efficient than normal conducting for some applications
- Still many topics to understand and improve current technology

- Gigi Ciovatti
- Rongli Geng
- Jean Delayen

References

-  H. Padamsee, J. Knobloch & T. Hays, *RF Superconductivity for Accelerators*, Wiley Series in Beam Physics and Accelerator Technology, 1988.
-  H. Padamsee, *SRF Technology*, Wiley Series in Beam Physics and Accelerator Technology.
-  A. Gurevich, *Superconducting Radio-Frequency Fundamentals for Particle Accelerators*, Reviews of Accelerator Science and Technology Vol.5 , 2012.
-  C. Reece, G. Ciovatti, *Superconducting Radio-Frequency Technology and Future Accelerator Applications*, Reviews of Accelerator Science and Technology Vol.5 , 2012.
-  M. Kelley *Superconducting RF Cavities*, Reviews of Accelerator Science and Technology Vol.5 , 2012.
-  Lectures from USPAS SRF Winter 2015 and Summer 2015.